Tracking the Heavy Metal Contaminants Entrained with the Flow into a Trickle Bed Hydrotreating Reactor Packed with Different Catalyst Shapes using Newly Developed Noninvasive Dynamic Radioactive Particle Tracking

Binbin Qi

Omar Farid

Alexandre França Velo

Jihane Mendil

et. al. For a complete list of authors, see https://scholarsmine.mst.edu/che_bioeng_facwork/1058

Chemical Engineering Journal 429 (2022) 132277

Contents lists available at ScienceDirect

Chemical Engineering Journal

journal homepage: www.elsevier.com/locate/cej

Tracking the heavy metal contaminants entrained with the flow into a Trickle bed hydrotreating Reactor packed with different catalyst shapes using newly developed noninvasive Dynamic radioactive particle Tracking

Binbin Qi [a], Omar Farid [a], Alexandre França Velo [c], Jihane Mendil [a,e], Sebastián Uribe [a], Yasunobu Kaneko [d], Kei Sakakura [d], Yasuhito Kagota [d], Muthanna Al-Dahhan [a,b,e,*]

[a] Multiphase flow and Reactor Engineering, Applications and Education Laboratory (mFReael), Linda and Bipin Doshi Department of Chemical and Biochemical Engineering, Missouri University of Science and Technology, Rolla, MO 65409, USA
[b] Department of Nuclear Engineering and Radiation Science, Missouri University of Science and Technology, Rolla, MO 65409, USA
[c] Radiology & Biomedical Imaging, Yale University, New Haven, CT 06520, USA
[d] Technology & Engineering Center, Idemitsu Kosan Co., Ltd., Chiba 261-7134, Japan
[e] Mohammed VI Polytechnic University, Lot 660, Hay Moulay Rachid 43150, Ben Guerir, Morocco

A R T I C L E I N F O

Keywords:
Trickle Bed Reactors
Heavy metal contaminants
RPT
Kernel Density Estimation

A B S T R A C T

A newly developed modified Dynamic Radioactive Particle Tracking system (DRPT) was used to investigate the heavy metal contaminants deposition locations in different catalyst beds, sphere, cylinder, trilobe, and quadrilobed in Trickle Bed Reactors. In the present paper, Kernel Density Estimator (KDE) was used to estimate the probability density distributions of heavy metal contaminants depositions in terms of bed radius height. The result shows that the four cases have similar probability density distribution in terms of radius, while the spherical catalyst has the larger distribution range in terms of bed height. The heavy metal deposition is directly related to the pressure drops along the bed height which indicate the bed porosity and intricate bed structure in catalyst packed beds. Heavy metals have more chance to deposit at higher levels of packed beds with higher pressure drops.

Nomenclature

d Dimensions of multivariate KDE
d_e Volumetric equivalent diameter
h Bandwidth of KDE
K Kernel density function
n Total sample number
X_i value of ith observation
$\langle v_i \rangle [m/s]$ Superficial average velocity vector of phase i
Greek symbols
β Gas phase
$\Delta P [Pa]$ Pressure drop
ε_i Holdup (volume fraction) of phase i
ε_B Bed porosity
φ Sphericity
γ Liquid phase
$\rho_i [kg/m^3]$ Density of phase i

1. Introduction

Trickle Bed Reactors (TBR) are the most used gas–liquid-solid interacting equipment in various processing such as petroleum hydrotreating processing (hydrodesulfurization, hydrodenitrification, hydrodemetallization, hydrocracking, etc.), hydrogenation reactions, oxidation reactions, esterification, as well as Fischer-Tropsch reactions [1]. In these processes, there are inevitably contaminants being delivered into the TBR, especially in hydroprocessing applications, where heavy residual oils are converted into lighter fuel oils. These contaminants (e.g., nickel, vanadium, arsenic, sodium, iron, lead) are usually associated with the produced crude oil, the remaining heavy metals in the liquid feed, or residues from the additives (silicon, lead) used during refining operations, as well as corrosion (iron) [2]. These contaminants directly or indirectly result in catalyst deactivation due to a chemical, mechanical, or thermal effect, such as poisoning, fouling, thermal

* Corresponding authors at: Multiphase flow and Reactor Engineering, Applications and Education Laboratory (mFReael), Linda and Bipin Doshi Department of Chemical and Biochemical Engineering , Missouri University of Science and Technology, Rolla, MO 65409, USA.
E-mail address: aldahhanm@mst.edu (M. Al-Dahhan).

https://doi.org/10.1016/j.cej.2021.132277
Received 1 March 2021; Received in revised form 30 August 2021; Accepted 1 September 2021
Available online 8 September 2021

Fig. 1. MiniCNC machine and micro drill bits.

degradation, or attrition [3] which leads to hot spots, high pressure drops, and even the need for emergency shutdowns. Currently , there is vast literature related to the catalysts aging, deactivation and regeneration including mechanisms and kinetical investigation [2–5]. All the work is in micro perspective that relies on the prerequisite that the contaminants already exist in the catalyst bed. There is no doubt that the contaminants are entrained through the liquid feed flow into the trickle beds hence get stuck and deposit. However, to the best of authors' knowledge, there is no such work that discloses how these contaminants are carried by the liquid fluid, the distribution of the deposition locations, and especially the effects of the catalyst bed structure, such as the catalyst shape, on the contaminant's deposition. Hence, in order to obtain insights into the interaction of the liquid fluid and the contaminant particles, and to provide guidance for industries to diagnose the common issues in TBRs such as hot spot or high pressure drops, it is essential to track the contaminants locations. The challenge of tracking the contaminants locations becomes more complex, since the size of the contaminants varies in a large range, from nanometer level to millimeter level, which precludes their visual identification, furthermore in the intricate interstitial space between the packing.

There have been various particle tracking methodologies reported in literature, which can aid in the identification of the contaminants' locations inside the packed beds. Single Particle Tracking (SPT) [6] is a methodology that uses computer-enhanced video microscopy to track the single particle motion in a system. However, it requires the system to be totally visible at least at the surface so that it can be captured by a camera. Laser Doppler Anemometry (LDA) and Particle Imaging Velocimetry (PIV) [7] are another two typical techniques to track particles. However, both techniques are optical methods based on the light reflection from the seeded particles hence tracking large amount of the particles to measure the velocity field in fluid dynamics. All these techniques are not feasible for the TBR system due to the impossible visual identification of the void space inside the bed. Hence, another non-invasive particle tracking technique that does not require the transparency or visibility, which is Radioactive Particle Tracking (RPT) [8–13], become a well-reasoned option. There are two types of RPT which are Static RPT (SRPT) and Dynamic RPT (DRPT). The SRPT aims to determine the Lagrangian trajectories, instantaneous and time averaged velocity field and various turbulent parameters (Reynolds stresses, turbulent kinetic energy, turbulent eddy diffusivities etc.) [9–13] based on a priori calibration data obtained when the tracer radioactive particle is placed statically inside the system under normal operation conditions. The tracer radioactive particle is made up of a gamma-ray isotope particle by either coating a layer with chemical and thermal resistant materials or embedding in a larger particle to match the substance density that needs to be measured depending on the system. The system is surrounded by an array of non-collimated scintillation (NaI (Tl)) detectors. Before the actual experiments, the SRPT system is calibrated by placing the isotope particle at various known positions under the desired operation to develop the correlation of counts in terms of distance for each detector. During the actual experiments, the instantaneous locations of the free moving particle can be reconstructed based on the correlation developed in the static calibration step, therefore the velocity field and various turbulent parameters can be found. Khane et al.

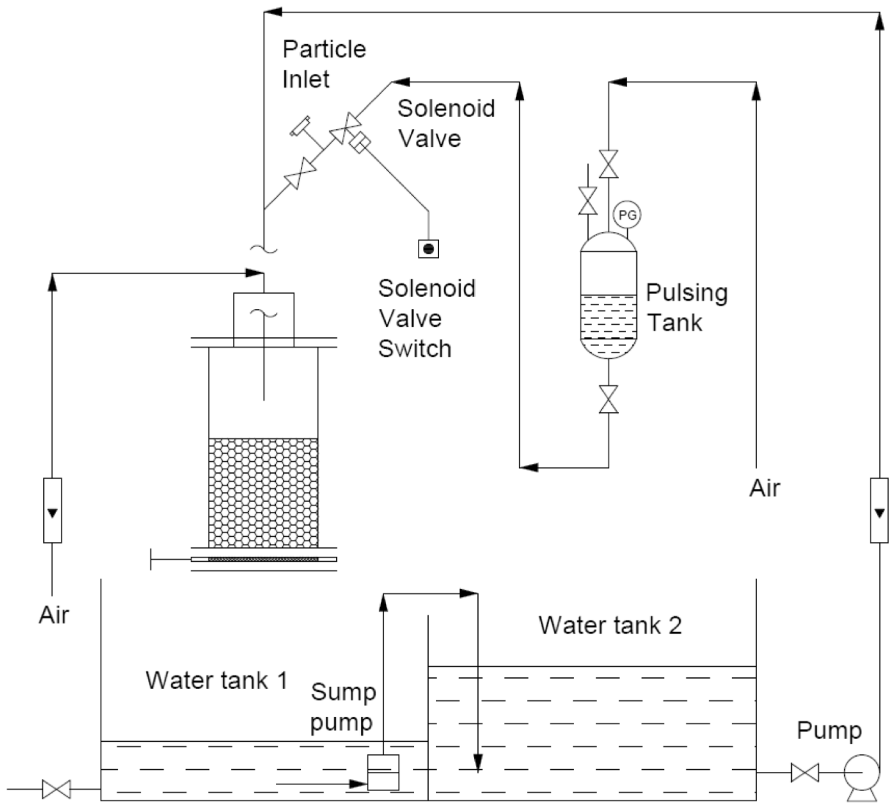

Fig. 2. Details of the experimental setup.

[8] developed a Dynamic Radioactive Particle Tracking (DRPT) to perform calibration for the RPT as a hybrid RPT system. The DRPT uses three moveable collimated scintillation (NaI (Tl)) detectors to seek the coordinate of the radioactive particle under motion. The main difference between these two RPT systems is that, SRPT tracks the trajectory of a dynamic object that is represented by the radioactive particle which mimics the moving phase to be tracked (liquid, solid), hence the Lagrangian trajectory is determined. From the Lagrangian trajectory, the velocity fields can be obtained and hence the fluctuation and turbulent parameters. While DRPT determines the location of a static object which is represented by the radioactive particle by dynamically moving the detectors to determine the coordinates of this object..

Therefore, in this work, the deposition locations of the heavy metal contaminants entrained through the liquid flow inside a TBR were investigated by a newly modified Dynamic Radioactive Particle Tracking system. According to our industrial collaborator, real contaminants have been collected and an average size of 500 μm is a reasonable representation for heavy metals in trickle bed reactors. It is worth to note here that the different catalyst shapes, sphere, cylinder, trilobe, and quadrilobed, have significant impacts on the flow behaviors inside a TBR [14–16]. Hence, these four catalyst shapes will be tested to identify the effects of the bed structure difference on the heavy metal contaminants deposition locations. Kernel Density Estimation (KDE) was used to determine the probability distribution of the contaminant final position, in terms of bed radius and height in each type of catalyst. This information can benefit not just industries to diagnose the common issues in TBRs such as contaminants deposition, hot spot or high pressure drop, it could also benefit the hydrodynamics investigation in Computational Fluid Dynamics (CFD) simulations as it provides valuable benchmarking data for CFD validation. The probability density information can be coupled with the packed bed porosity distribution function giving more realistic bed structure so that researchers can investigate the flow behaviour or hydrodynamics under the case of contaminant deposition which can be extended for the beds with catalyst coking or sintering scenarios when the bed structure can be determined or assumed.

2. Experimental setups

2.1. Radioactive particle representing the heavy metal contaminants

As mentioned earlier, the heavy metal contaminants could be any size and shape. In order to balance the maneuverability and representativeness, a spherical particle with 500 μm in diameter and 2000–3000 kg/m3 in density was considered to be used for the experiments. Therefore, a Co-60 ($\phi\,300\,\mu m$, 18.5 MBq ($500\,\mu Ci$), with main yield energies of 1173.2 keV and 1332.5 keV, 5.27 half-life years) radioactive particle was embedded in a PMMA particle ($\phi\,500\,\mu m$, 1200 kg/m^3). A MiniCNC machine with a 0.3 mm drill bit was used to drill the hole in the PMMA particle. The Co-60 particle was placed inside the hole of the PMMA particle under the microscope and then it was sealed with Epoxy glue. After drying out, the particle was spray painted with orange color in order to be easily found during the experiments. The tools that were used are shown in Fig. 1. The theoretical density (maximum) after the calculation is 2863.2 kg/m^3.

2.2. Trickle bed Reactor system

The schematic of the Trickle Bed Reactor (TBR) system is shown in Fig. 2. The TBR is made of an acrylic column which is 1 foot (30.48 cm) in height and 5.5 in. (13.97 cm) in inner diameter. At the bottom of the column, a mesh gate valve was used to support the catalyst pack bed and to enable water and air passing through freely with negligible pressure drop. This mesh gate valve can be opened easily to remove the catalysts from the column in order to fish the particle or clean the system. A single nozzle pipe with 9 mm inner diameter was used as liquid inlet while two gas inlets (9mminnerdiameter) were attached to the top flange to obtain better distribution. The bottom of the liquid inlet is 2 cm away from the

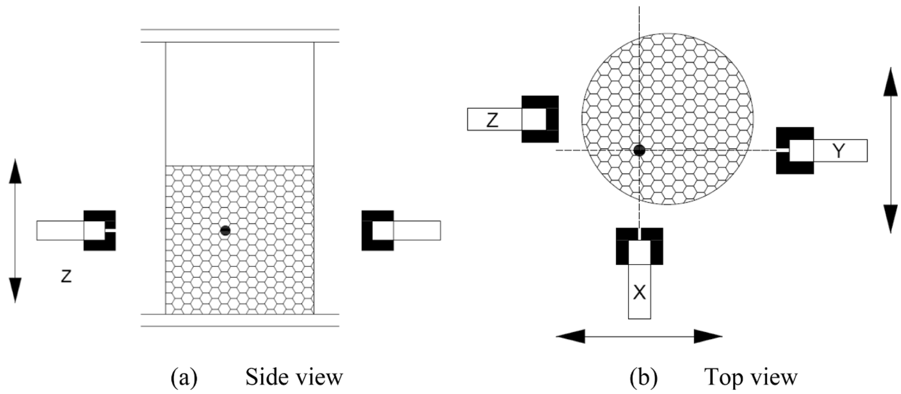

Fig. 3. Schematic of the Dynamic Radioactive Particle Tracking system.

top of the packed bed. Both liquid and gas flowrates were controlled by the flowmeters. A particle injection system was attached to the liquid inlet pipe with a Y connector. The full description and operation procedure of the particle injection system will be explained at length later. A water tank with two sections was used in order to prevent the radioactive particle from being sucked by the pump, in case that it had passed through the packed bed and drop inside the tank. A sump pump was used to help circulate the water in the system..

2.3. Particle injection system

The particle injection system includes a pressurized pulsing tank, a normally closed solenoid valve controlled by a switch, a particle inlet, and a normal valve. Before experiments, the pulsing tank will be filled with water up to about half of the tank. Then the high-pressure air will be injected into the pulsing tank to pressurize the tank to no more than 30 Psi (206.843 KPa) in order to minimize the effects on the inlet liquid flow. The normally closed solenoid valve can prevent the water getting inside the system unless the switch is turned on. After that, the radioactive particle will be placed inside the particle inlet. To avoid that the particle flows directly inside the system, the normal valve will not be open until running the gas and liquid flow.

2.4. Location identification system of Dynamic radioactive particle Tracking technique

The modified DRPT system uses 3 collimated Sodium Iodide (NaI (Tl), $\phi\,5 \times 5$ cm) scintillation detectors (Canberra Model 2007, named as X, Y, Z, respectively) to seek the coordinates of the radioactive particle. As shown in Fig. 3, X Y and Z detectors are located at the same level and can be moved vertically by a 2-phase stepping motor to locate the Z coordinate of the radioactive particle. X and Y detectors are driven by a 2-phase stepping motors to move horizontally. These two detectors are perpendicular to each other so that X and Y coordinates can be easily determined. It is noted that all the detector crystals are fully covered by the lead collimators only with narrow slots (0.1 cm wide, 5 cm long). For the Z detector, the slot in the collimator is horizontally oriented while for the X and Y detectors, the slots are vertically oriented. As the detectors move in discrete steps, the photon counts of all the detectors will be tracked and recorded for 30 s at each position. The data acquisition system consists of 3 timing filter amplifiers (Canberra 2111), a channel discriminators (PhillipsScientific, CAMAC Model 7106, 32 channels), 225 MHz scalers(Phillips Scientific, CAMAC Model 7132H, 32 channels), and CC-USB CAMACcontroller (W-IE-NER). The operation procedure and validation of this system will be described in the following section.

Table 1
Geometrical properties of the solid particles and bed.

Shape	ε_B	$d_e[mm]$	φ	Actual size [mm]
Spheres	0.36	4.7	1	4.7
Cylinders	0.451	4.13	0.82	5.5 × 3
Trilobes	0.526	3.93	0.62	6 × 3
Quadrilobes	0.544	3.35	0.72	6 × 2.5

Where ε_B is bed porosity, d_e is volume equivalent diameter, φ is sphericity.

3. Procedure and validation

3.1. Experimental procedure

The complete experimental procedure is summarized in the flowchart below shown in Fig. 4.

(1) Bed packing

Four types of catalysts, sphere, cylinder, trilobe, and quadrilobed,

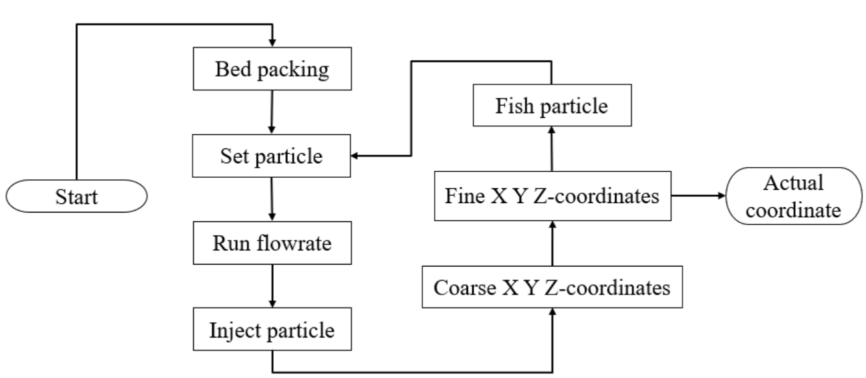

Fig. 4. Flowchart of experimental procedure.

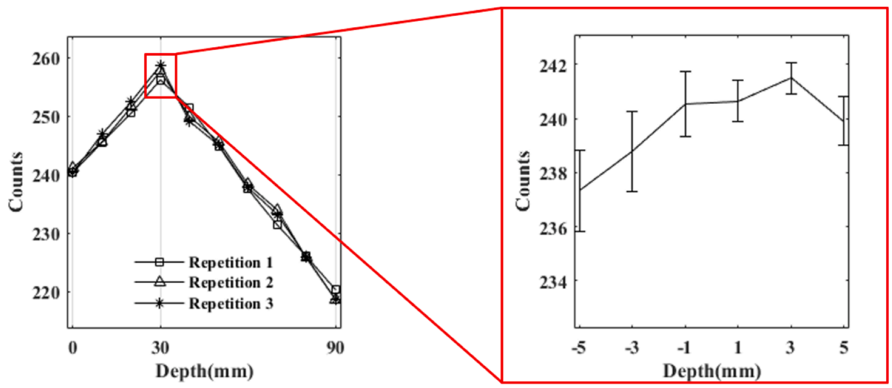

(a) Coarse seeking (b) Fine seeking

Fig. 5. Sample results of coarse seeking and fine seeking procedure.

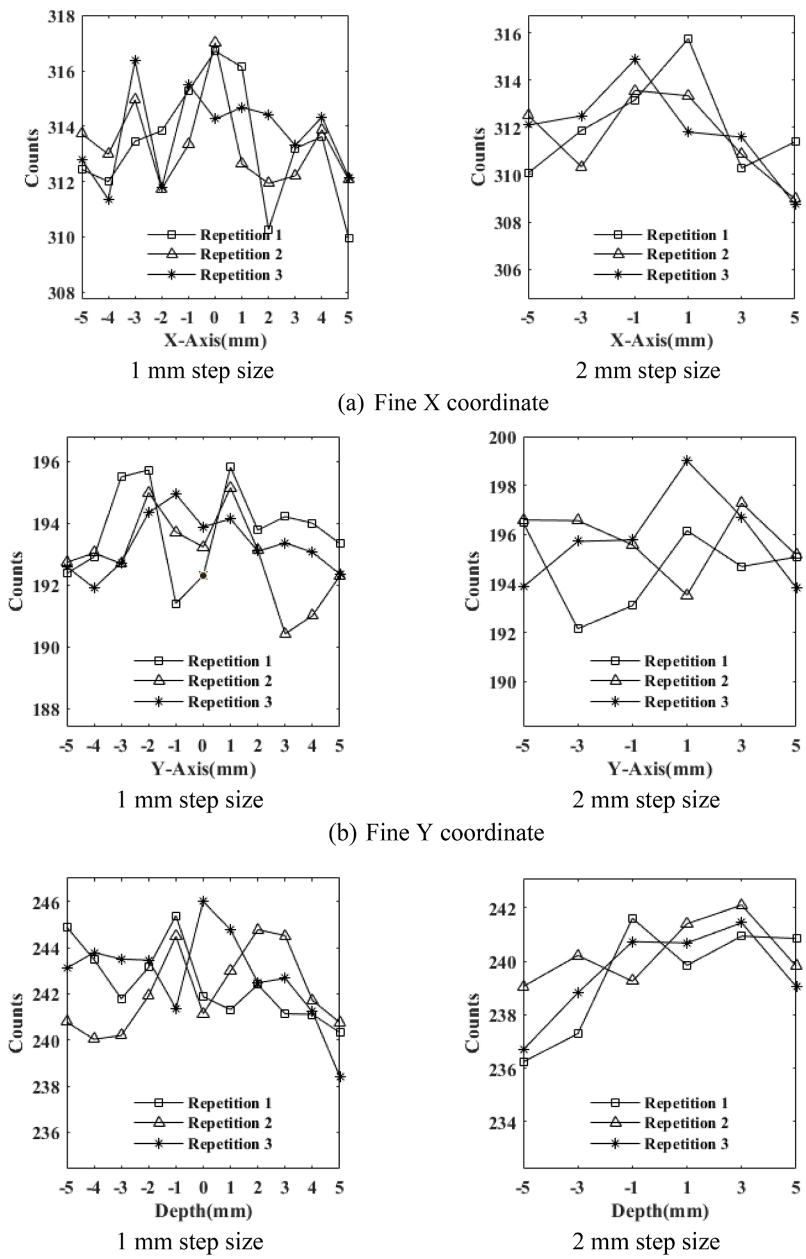

1 mm step size 2 mm step size
(a) Fine X coordinate
1 mm step size 2 mm step size
(b) Fine Y coordinate
1 mm step size 2 mm step size
(c) Fine Z coordinate

Fig. 6. Comparisons between 1 mm and 2 mm step sizes for fine coordinates seeking.

were used in this work. The geometrical characteristics [14,16] of these catalysts and the packed beds are listed in Table 1. The purpose of this work is to assess the impacts of different catalyst shapes on heavy metal contaminants deposition. Hence, the gas and liquid flowrates are the same for all tested catalyst shapes. The packed bed was set to be 15 cm in height, by virtue of preliminary experiments that showed that the 500 μm radioactive particle almost had no chance to pass through a packed bed of such height for all the catalyst shapes.

(2) Setting the particle

Before running the gas and liquid flow, the radioactive particle will be placed inside the particle inlet in the particle injection system as explained earlier. During this step, the normal valve should always be kept closed to prevent the particle from dropping inside the packed before it is injected. After putting the particle inside the inlet, the gamma-ray survey meter will be used to check if the particle is at the right place.

(3) Running the flowrate

The air valve is open and the superficial velocity is set at 0.05 m/s, later on the water pump is turned on and the superficial velocity is set at 0.0065 m/s. The system is kept running for 5 min in order to stabilize the flow of air and water into the trickle bed.

(4) Injecting the particle

The normal valve on the particle injection line is then opened, and the solenoid valve switch is quickly pressed to enable the pressurized water to push the particle into the system in a very short time to minimize the effect on the system. The gas/liquid flowrates are kept running for another 5 min before turning off the pump and air flow.

(5) Identifying the coarse X Y Z-coordinates of the particle location (coarse seeking coordinates)

The particle location seeking procedure is divided into two steps, coarse seeking and fine seeking coordinates. For coarse seeking coordinates, the step size is 1 cm. In Z direction, starting from the top of the packed bed and moving downward, the detector will collect the counts at each centimeter for 30 s until reaching the 14 cm-depth that there are total 15 data points. The coarse position at Z-axis can be determined from the data plot that the point has the highest counts should be the coarse Z coordinate as shown in Fig. 5 **(a)**. Then the collimated detectors of the DRPT system will be moved up to that particular position (highest counts) for X and Y coordinates seeking. Since the TBR column has 5.5 in. (13.97 cm) inner diameter and 6 in. (15.24 cm) outer diameter, 15 cm horizontal moving range is enough for the X and Y detectors to cover the whole column diameter in X and Y directions. Similarly, starting from the left edge, the X and Y detectors will collect counts at each centimeter for 30 s until reaching the right edge that total 15 data points will be generated to obtain the peak, therefore the coarse X and Y coordinates.

(6) Identifying the fine X Y Z- coordinates of the particle location (fine seeking coordinates

Once the coarse coordinates are found, all the detectors will be moved to their coarse coordinates as the base reference to seek the fine coordinates. The reference coarse coordinates plus and minus 5 mm will be the moving range (Fig. 5**(b)**). By recalling that the slots on the collimators covering the detectors are 1 mm wide and 5 cm long. It is reasonable to make the initial assumption of the step size as 1 mm for fine seeking. However, from the plots in Fig. 6, the indication of a peak is quite ambiguous for 1 mm step size, which cannot be used to identify the fine coordinates. Therefore, 2 mm step size was assessed by following the same procedure. In this way, clear indications of peaks can be identified. In order to minimize the error and achieve the repeatability and reproducibility, three repetitions of data collections are conducted, hence pinpointing the fine coordinates by averaging the 3 repetition results. Based on the plot of the average of 3 repetitions and error bars, the fine X Y and Z coordinates can be located with tolerance of ± 1 mm.

(7) Determining the actual coordinate

From the coarse seeking and fine seeking coordinates, the actual coordinate can be determined. For example, in Fig. 5, the coarse depth of

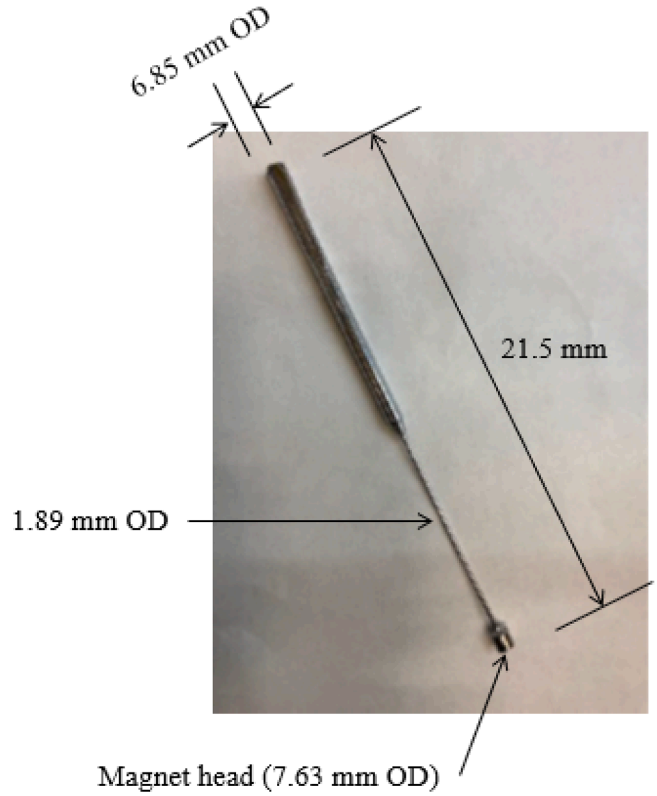

Fig. 7. Magnetic fishing tool.

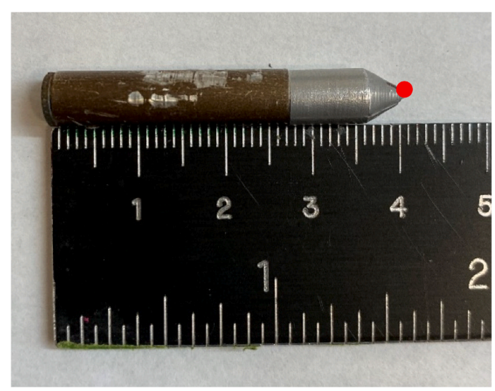

Fig. 8. Co-60 in a capsule.

the radioactive particle is 30 mm from the top of the packed bed. From the fine seeking coordinate ranging in 25 – 35 mm, it can be seen that at + 3 mm position it has the highest counts with minimum error bar. Hence, the actual coordinate (depth) of Z direction would be 33 ± 1 mm.

(8) Fishing the particle

A fishing tool with a magnetic head (7.63 mm in diameter, Fig. 7) is used to fish the radioactive particle since the Co-60 is magnetic. From the actual coordinates obtained from coarse and fine seeking coordinates, it is easy to locate and insert this tool inside the packed bed to fish the particle. The advantage of this tool is that there is no necessary to remove all the catalysts and load them again. In this way, it is able to minimize the disturbance to the packed bed configuration. However, sometimes when the particle goes very deep inside the packed bed, where it is very difficult to use the fishing tool, removing all the catalysts from the bottom by opening the mesh gate valve would be a better option. After that, the whole procedure will be repeated for the next experiment.

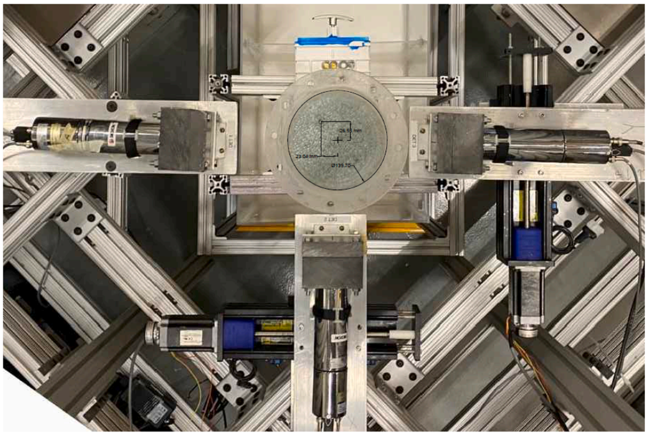

Fig. 9. Top view picture of validation.

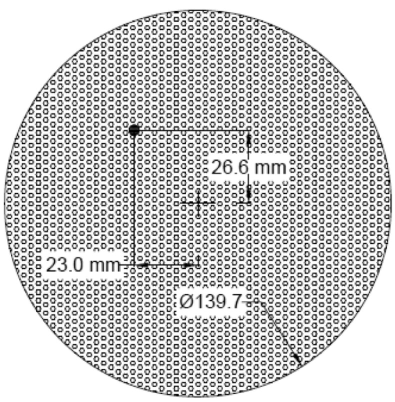

(a) Top view of the schematic of the Co-60 location

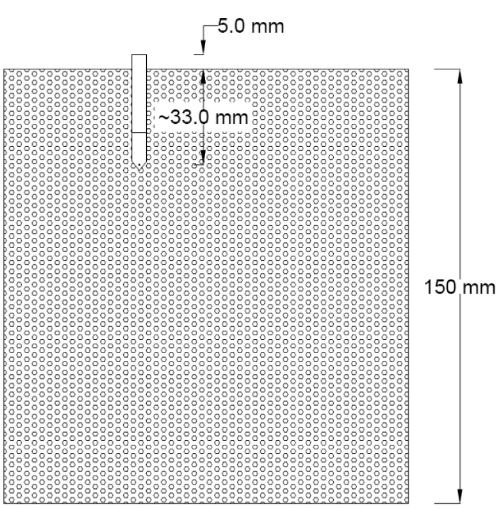

(b) Side view of the schematic of the Co-60 location

Fig. 10. Schematic of the Co-60 location for validation.

3.2. *Validation of the location identification system of Dynamic radioactive particle Tracking technique*

Validation of the capability and reliability, as well as the accuracy is always necessary for a newly developed experimental system. In order to validate the newly developed DRPT system, the Co-60 particle was placed in a known location by putting it a capsule as shown in Fig. 8. The

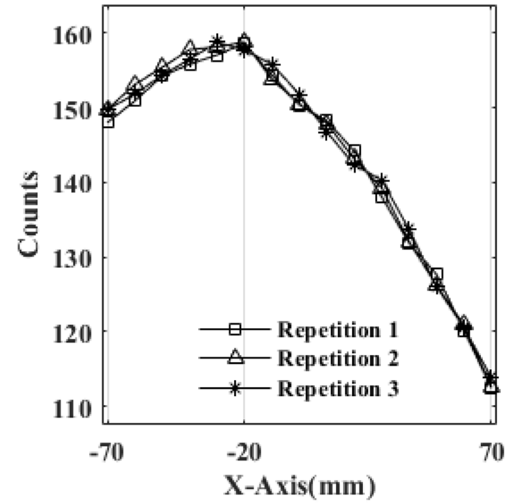

(a) Coarse X coordinate

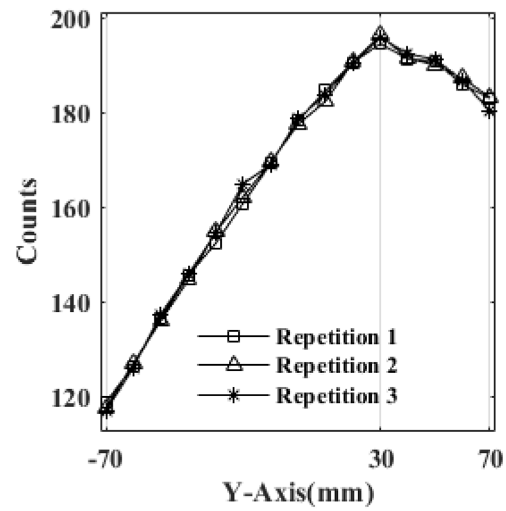

(b) Coarse Y coordinate

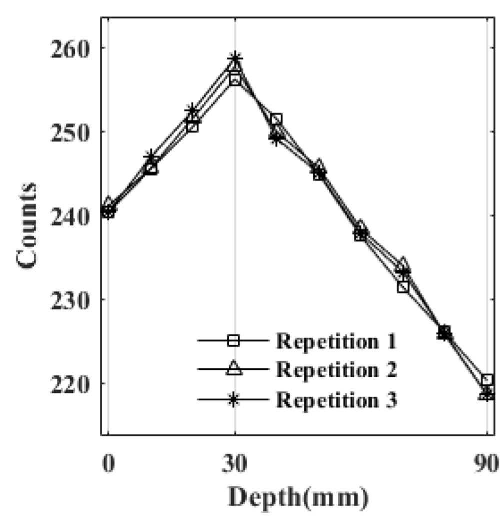

(c) Coarse Z coordinate

Fig. 11. Coarse coordinates of the Co-60 location for validation.

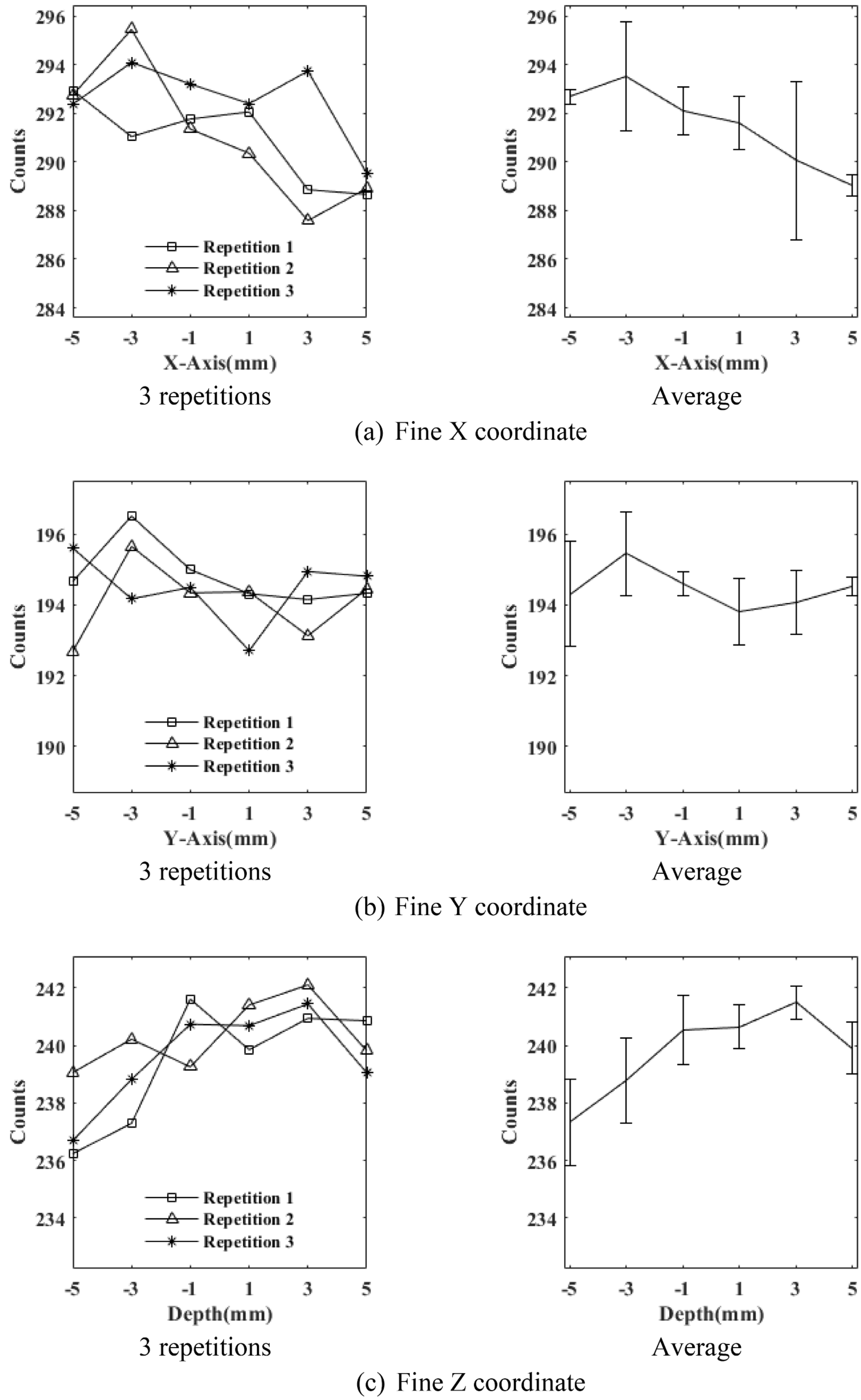

Fig. 12. Fine coordinate of the Co-60 particle with 2 mm step size before and after averaging.

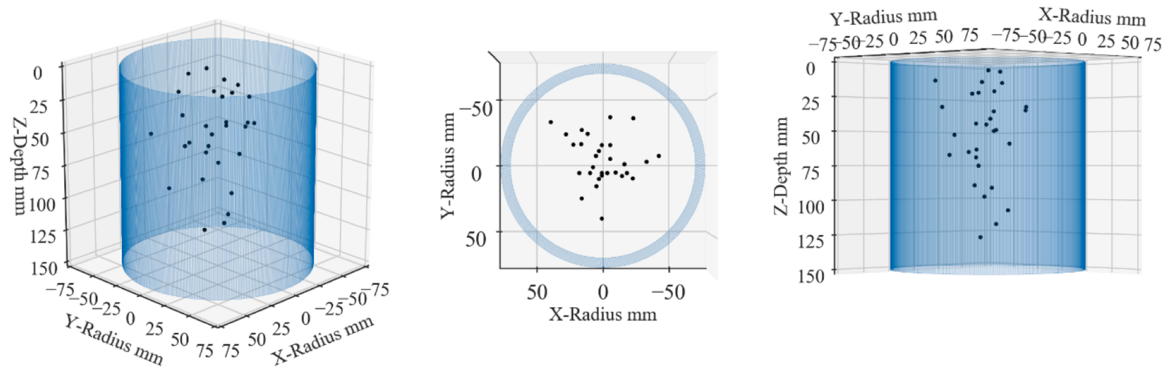

(a) Particle distribution inside spherical catalyst bed

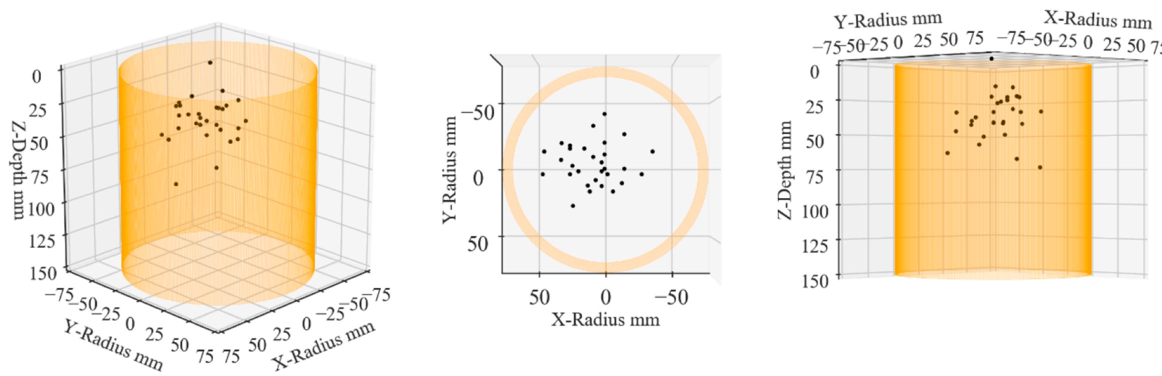

(b) Particle distribution inside cylindrical catalyst bed

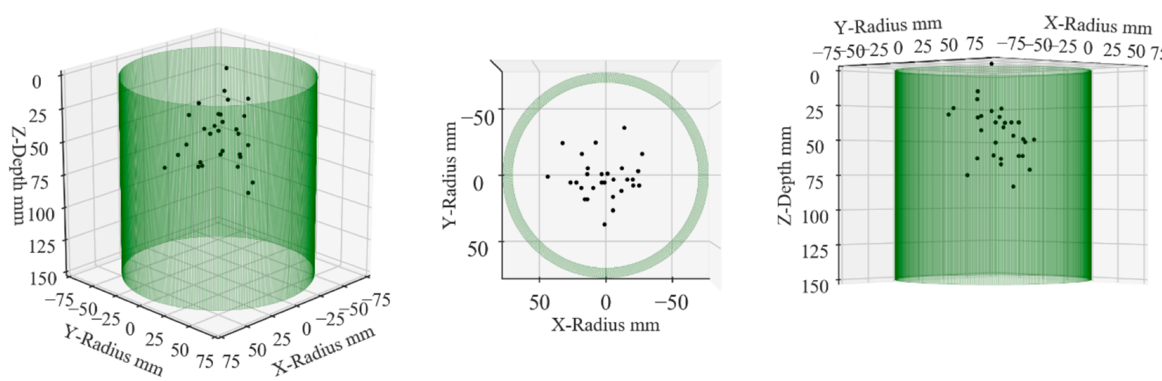

(c) Particle distribution inside trilobe catalyst bed

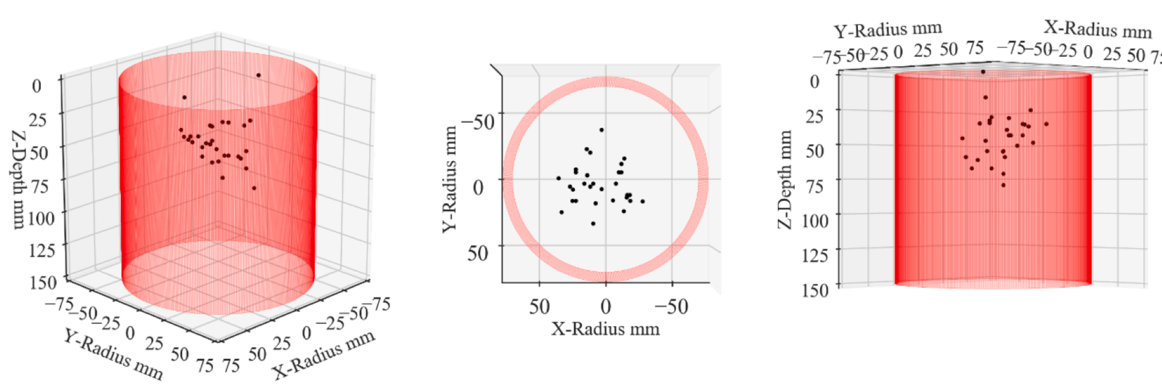

(d) Particle distribution inside quadrilobe catalyst bed

Fig. 13. Particle distribution insdie different catalyst beds.

Table 2
Kernel density functions.

Name	$K(x)$
Epanechnikov	$\frac{3}{4}\left(1-\frac{1}{5}x^2\right)\Big/\sqrt{5}\text{for}\|x\|<\sqrt{5}$ 0 otherwise
Biweight	$\frac{5}{6}(1-x^2)^2\text{for}\|x\|<1$ 0 otherwise
Triangular	$1-\|x\|\text{for}\|x\|<1$ 0 otherwise
Gaussian	$\frac{1}{\sqrt{2\pi}}exp-\frac{1}{2}x^2$
Rectangular	$\frac{1}{2}\text{for}\|x\|<1$ 0 otherwise

capsule is around 4 cm long and the Co-60 particle is located at around 38 mm due to the thickness of the tip. The capsule was vertically inserted into the bed at a random location with around 5 mm left above the top line of the bed for better visualization and taking a picture. Based on the picture (Fig. 9) that was taken from the top view, with AutoCAD it can be found that the actual coordinate of the Co-60 particle is [–23, 26.6, 33] mm as shown in Fig. 10.

For validation, even coarse seeking coordinate step was repeated 3 times to show the accuracy of the system as shown in Fig. 11. All 3 repetitions give exact the same coarse coordinate which is [-20, 30, 30] mm. In view of this, it is not necessary to repeat 3 times for the coarse seeking coordinate steps during real experiments. The fine coordinate of the Co-60 particle is [-3, −3, 3] mm as shown in Fig. 12. By combining the coarse and fine coordinates, the actual coordinate of the Co-60 particle for validation is [-23 ± 1, 27 ± 1, 33 ± 1] mm, which is solid validation of the newly developed DRPT system.

4. Results and discussion

For each catalyst shape, 30 experiments were repeated by following the procedure described in the previous section. All the coordinates of the heavy metal deposition locations are projected in the 3D plots as shown in Fig. 13. It can be observed that all catalyst shapes have similar radius distribution, while spherical catalyst has larger axial distribution range. The final locations of the heavy metals are totally random due to the unpredicted flowing paths inside random packed bed, which in other words, the deposition locations are in total uncertainties. In order to characterize this uncertain data due to the randomness of this experimental work, probability density distribution was estimated based on the results. There are two statistical analysis methodologies which are parametric and nonparametric procedures [17]. Parametric analysis is based on large amount of sample data which can give the statistical parameters such as mean, standard deviation, and variance. In other words, the parametric analysis assumes that data is normally distributed. However, nonparametric analysis has no assumption about the population, which is not based on the parameters of a normal distribution. The most common way to do nonparametric estimation is the histogram. However, the histogram has difficulties to represent smooth continuous function and bivariate or trivariate data [18]. Therefore, in this work, Kernel Density Estimator (KDE) [18,19] was used to estimate the probability density distribution as a continuous function, which is feasible for small population as in such work. The KDE is defined as Equation (1):

$$f(x)=\frac{1}{nh^d}\sum_{i=1}^{n}K\left(\frac{x-X_i}{h^d}\right)$$

Where n is the total sample number, h^d is the bandwidth for d dimensions multivariate KDE, K is the kernel density function and the common ones are listed in Table 2, X_i is the value of ith observation.

In this case, the Gaussian kernel density function was used as plotted in Fig. 14. The probability density distributions of four catalyst shapes are quite similar to the observation.

In terms of radius, all of them have similar probability density distribution and the highest probability is at around $r=20$ mm. In terms of height, spherical catalyst has larger distribution range than the other types do. However, all of them have the highest probability at around $z=50$ mm. Recalling the bed porosity of each catalyst shape in Table 1, spherical shape has the lowest bed porosity while trilobe and quadrilobe shapes have similar bed porosity, which means, theoretically the heavy metal should have more chance to pass through and deposit at lower locations in the trilobe or quadrilobe beds, however, the experimental data indicate otherwise. The particles get stuck in a higher position in extrudate catalysts (tri, quad, cylinders), because the void space distribution is more tortuous. This means, the free paths for the particle to flow through are more intricate. In spherical catalyst, such free paths are longer and less intricate. Therefore, the void space distribution on a bed packed with spheres is less tortuous. An indicative of the tortuosity and the intricate of such porous matrix can be found to be related to the pressure drop. Al-Ani et al. [16] investigated the effects of all these 4 catalyst shapes on the pressure drop and liquid holdup in a 6 in. TBR, indicating that spherical shape has the lowest liquid holdup and pressure drop along the bed height while the other shapes have similar holdups and pressure drops as shown in Fig. 15. Extruded catalysts have a higher pressure drop, which is physically explained due to the fact that these shapes provide higher resistances for the liquid to flow (because of the intricate porous structure). Hence, it can be observed that an insight into the contaminants final position in a TBR can be obtained by looking at tortuosity of the bed, which can be inferred by the pressure drop of the system and the bed structure and porosity. The reason why all catalyst shapes have similar radial probability density distributions can be explained similarly. When liquid flows inside the cylindrical, trilobe and quadrilobe beds, due to the random packing, the horizontal oriented catalysts act as guides leading the water to disperse further in the radial direction. However, because of high pressure drop, in other words, high momentum loss, the liquid velocity (kinetic energy) is not high enough to push the particle sideways. When the liquid flows inside the spherical bed, since there are no horizontal guides leading water to flow sideways, the liquid flows along the least resistant path. However, because of the compact structure of spheres which leads to low porosity, it is hard for the particle to pass through the little space among these spherical catalysts. Instead, the liquid wave might be able to push the particle away from the center towards to the wall until reaching the maximum liquid distribution location. Therefore, the combination of pressure drop and tortuosity determine the phenomena showing in the results.

5. Remarks

We have developed a new method to seek the coordinates of the radioactive particle mimicking the heavy metal deposition inside a Trickle Bed Hydrotreating Reactor, using a modified Dynamic Radioactive Particle Tracking system (DRPT). The resolution obtained by the coarse and fine coordinates is high enough to clearly identify the location of the radioactive particle and to validate the capacity and reliability of this newly developed DRPT system. We have identified the location of the radioactive using a study on different catalysts shapes by accurately determining:

(1) The probability density distributions by using Kernel Density Estimator (KDE). The results show that in terms of:
- Radius: all the catalysts have similar probability density distribution, and the highest probability is at around $r=20$ mm.
- Height: the spherical catalyst has larger distribution range than the other types do.

(2) The heavy metal deposition is directly related to the pressure drops along the bed height which indicate the bed porosity and intricate bed structure in catalyst packed beds. Heavy metals

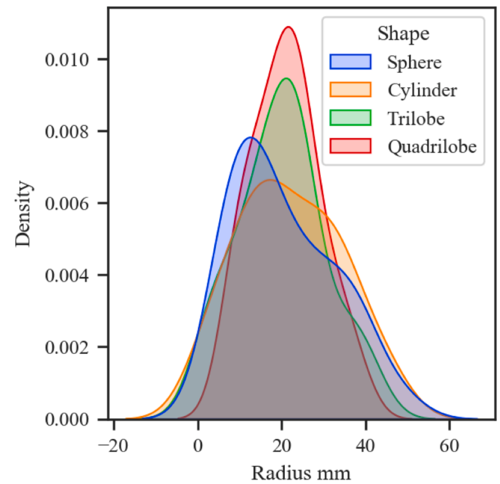

(a) Kernel density estimation of heavy metal deposition locations in terms of radius

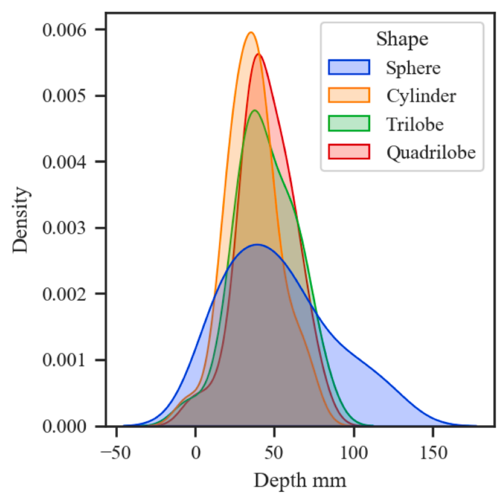

(b) Kernel density estimation of heavy metal deposition locations in terms of depth

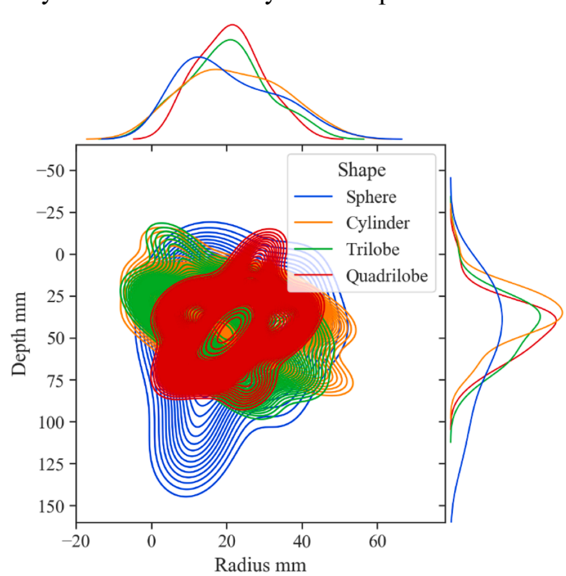

(c) Jointplot of Kernel density estimation of heavy metal deposition locations

Fig. 14. Kernel density estimation of heavy metal deposition locations.

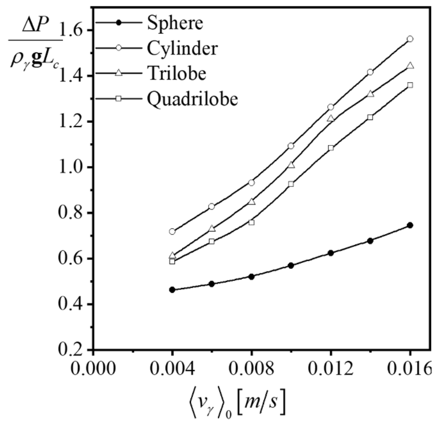

(a) Pressure drop in different catalyst beds at gas velocity 0.06 m/s [16]

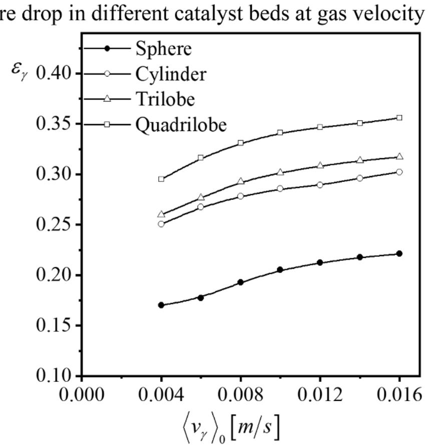

(b) Liquid holdup in different catalyst beds at gas velocity 0.06 m/s

Fig. 15. Pressure drop and liquid holdup in different catalyst beds for various liquid velocities at gas velocity 0.06 m/s [16].

have more chance to deposit at higher levels of packed beds with higher pressure drops for the extrudate catalyst shapes such as cylinder, trilobe, and quadrilobed.

Funding

This research did not receive any specific grant from funding agencies in the public, commercial, or not-for-profit sectors.

Declaration of Competing Interest

The authors declare that they have no known competing financial interests or personal relationships that could have appeared to influence the work reported in this paper.

References

[1] V. V. Ranade, R. V. Chaudhari, P.R. Gunjal, Introduction, Trickle Bed React. React. Eng. Appl. (2011) 1–23. https://doi.org/10.1016/b978-0-444-52738-7.10001-4.

[2] P. Dufresne, Hydroprocessing catalysts regeneration and recycling, Appl. Catal. A Gen. 322 (2007) 67–75, https://doi.org/10.1016/j.apcata.2007.01.013.

[3] M.D. Argyle, C.H. Bartholomew, Heterogeneous catalyst deactivation and regeneration: A review, Catalysts. 5 (2015) 145–269, https://doi.org/10.3390/catal5010145.

[4] P.W. Tamm, H.F. Harnsberger, A.G. Bridge, Effects of Feed Metals on Catalyst Aging in Hydroprocessing Residuum, Ind. Eng. Chem. Process Des. Dev. 20 (2) (1981) 262–273, https://doi.org/10.1021/i200013a014.

[5] B.M. Vogelaar, S. Eijsbouts, J.A. Bergwerff, J.J. Heiszwolf, Hydroprocessing catalyst deactivation in commercial practice, Catal. Today. 154 (3-4) (2010) 256–263, https://doi.org/10.1016/j.cattod.2010.03.039.

[6] M.J. Saxton, K. Jacobson, Single-particle tracking: Applications to membrane dynamics, Annu. Rev. Biophys. Biomol. Struct. 26 (1) (1997) 373–399, https://doi.org/10.1146/annurev.biophys.26.1.373.

[7] H.G. Maas, A. Gruen, D. Papantoniou, Particle tracking velocimetry in three-dimensional flows - Part 1. Photogrammetric determination of particle coordinates, Exp. Fluids. 15 (2) (1993) 133–146, https://doi.org/10.1007/BF00190953.

[8] V. Khane, M.H. Al-Dahhan, Hybrid dynamic radioactive particle tracking (RPT) calibration technique for multiphase flow systems, Meas. Sci. Technol. 28 (5) (2017) 055904, https://doi.org/10.1088/1361-6501/aa5c27.

[9] V. Khane, I.A. Said, M.H. Al-Dahhan, Experimental investigation of pebble flow dynamics using radioactive particle tracking technique in a scaled-down Pebble Bed Modular Reactor (PBMR), Nucl. Eng. Des. 302 (2016) 1–11, https://doi.org/10.1016/j.nucengdes.2016.03.031.

[10] V.B. Khane, M.H. Al-Dahhan, Study of solids movement in pebble bed/moving bed reactors using radioactive particle yracking (RPT) technique, in: 7th World Congr. Ind. Process Tomogr., 2014.

[11] V. Khane, I.A. Said, M.H. Al-Dahhan, Assessment of performing experimental investigation on a pebble bed modular reactor (PBMR) as a static packed bed approximation, Ann. Nucl. Energy. 101 (2017) 339–346, https://doi.org/10.1016/j.anucene.2016.11.020.

[12] M.K. Al Mesfer, A.J. Sultan, M.H. Al-Dahhan, Study the effect of dense internals on the liquid velocity field and turbulent parameters in bubble column for Fischer-Tropsch (FT) synthesis by using Radioactive Particle Tracking (RPT) technique, Chem. Eng. Sci. 161 (2017) 228–248, https://doi.org/10.1016/j.ces.2016.12.001.

[13] T. Al-Juwaya, N. Ali, M. Al-Dahhan, Investigation of hydrodynamics of binary solids mixture spouted beds using radioactive particle tracking (RPT) technique, Chem. Eng. Res. Des. 148 (2019) 21–44, https://doi.org/10.1016/j.cherd.2019.05.051.

[14] B. Qi, S. Uribe, O. Farid, M. Al-Dahhan, Development of a hybrid pressure drop and liquid holdup phenomenological model for trickle bed reactors based on two-phase volume averaged equations, Can. J. Chem. Eng. 99 (8) (2021) 1811–1823, https://doi.org/10.1002/cjce:v99.810.1002/cjce:23892.

[15] B. Qi, O. Farid, S. Uribe, M. Al-Dahhan, Maldistribution and dynamic liquid holdup quantification of quadrilobe catalyst in a trickle bed reactor using gamma-ray computed tomography: Pseudo-3D modelling and empirical modelling using deep neural network, Chem. Eng. Res. Des. 164 (2020) 195–208, https://doi.org/10.1016/j.cherd.2020.09.024.

[16] M. Al-Ani, M. Al-Dahhan, Effect of catalyst shape on pressure drop and liquid holdup in a pilot plant trickle bed reactor, Fuel. 284 (2021) 118860, https://doi.org/10.1016/j.fuel.2020.118860.

[17] D.J. Sheskin, Parametric and non parametric statistical procedures, Third edition, 2003.

[18] U. Diwekar, A. David, BONUS Algorithm for Large Scale Stochastic Nonlinear Programming Problems, 2015.

[19] B.W. Silverman, Density estimation: For statistics and data analysis, 2018. https://doi.org/10.1201/9781315140919.